SYNTHESIS AND SINTERING 3 (2023) 88–106

Available online at www.synsint.com

Synthesis and Sintering

ISSN 2564-0186 (Print), **ISSN** 2564-0194 (Online)

Research article

Sensitivity analysis of fluid flow parameters on the performance of fully dense ZrB_2-made micro heat exchangers

Mohsen Naderi [a], **Mohammad Vajdi** [a,*], **Farhad Sadegh Moghanlou** [a], **Hossein Nami** [b]

[a] *Department of Mechanical Engineering, University of Mohaghegh Ardabili, Ardabil, Iran*

[b] *SDU Life Cycle Engineering, Department of Green Technology, University of Southern Denmark, Campusvej 55, Odense M 5230, Denmark*

ABSTRACT

Heat exchangers are important in modern technology and are used in various industries such as power plants, automobiles, and airplanes. Their main role is to ensure efficient heat transfer tailored to specific system needs. With miniaturized electronics, challenges such as circuit overheating have emerged, increasing the demand for compact yet high-performance heat exchangers. The advent of micro-electromechanical systems has increased the application of micro heat exchangers with their high surface-to-volume ratio, promising enhanced efficiency. Although metals such as aluminum are commonly used for fabricating heat exchangers, their susceptibility to corrosion and high temperatures limits their usefulness. This study turns attention to ultrahigh temperature ceramics, specifically fully sintered ZrB_2, known for their high-temperature durability and oxidation resistance. Utilizing the Taguchi approach, a robust optimization method, this study explores the sensitivity analysis of fluid flow parameters on the performance of fully dense ZrB_2-made micro heat exchangers and highlights the potential of ceramics in heat exchanger construction.

KEYWORDS

Micro heat exchangers
ZrB_2
Taguchi method
ANOVA
Heat transfer
Pressure drop

OPEN ACCESS

1. Introduction

In the modern and industrialized world, heat exchangers play a vital role. They are an essential element in a wide variety of engineering applications, including power plants, automobiles, aircraft, process and chemical industries, and heating, air conditioning, and refrigeration systems. These facilities are optimized to provide an efficient and economical heat transfer between two or more materials according to specific process or system requirements [1–3].

Heat exchangers can be classified into two main direct and indirect contact categories based on the contact way between warm and cold fluids. In addition, according to the direction of fluid flow, they can be categorized into groups such as counter flow, parallel flow, and cross flow, and geometrically, they are also classified into several different categories, including tubular, plate, and developed plates [2]. The surface-to-volume ratio is one of the important components in the definition and classification of heat exchangers. Especially in the field of compressed or non-compressed heat exchangers, this parameter is essential [4].

Due to the miniaturization trend, especially in electronics, problems such as overheating of electronic circuits have emerged. Such problems have increased the demand for small and high-efficiency heat exchangers [5]. To solve the problem of cooling with high flux and small dimensions, and with recent developments in the field of micro-electro-mechanical systems (MEMS), micro heat exchangers have also been proposed as a new chapter in this field [6]. On the other hand, heat exchangers with small or miniature dimensions have been noticed due to their high surface-to-volume ratio. These novel heat exchangers, with the ability to transfer heat flux up to 790 W/cm^2, reduce the size of devices and increase their efficiency [4].

The effectiveness of heat exchangers, which is defined based on the second law of thermodynamics, is one of the main criteria for

* Corresponding author. *E-mail address:* vajdi@uma.ac.ir (M. Vajdi)

Received 24 February 2023; Received in revised form 26 April 2023; Accepted 27 April 2023.

https://doi.org/10.53063/synsint.2023.32143

evaluating their performance. The effectiveness depends on several factors, including the general heat transfer coefficient. This parameter, which is inversely defined by the sum of thermal resistances, is a function of the fluid convection coefficient and the conductive resistance of the wall [7]. In general, metals with high thermal conductivity, such as aluminum, are used to construct heat exchangers. However, this metal is not useful at high temperatures, and in addition, it has no resistance against corrosive fluids and can be affected by corrosion [8]. In this case, using ceramics resistant to temperature and corrosion can be a suitable alternative [9].

One of the important and prominent features of high-temperature ceramics is their thermal conductivity coefficient. Some of these materials, such as ZrB_2, TiB_2, and Si_3N_4, have higher thermal conductivity than some ferrous alloys. This characteristic has made them appropriate for special applications such as high-temperature heat exchangers [10–13]. Zirconium diboride is an ultrahigh-temperature ceramic that has been mostly noted for its outstanding thermal properties and resistance against oxidation at high temperatures. This ceramic has a very high melting point (~3245 °C) and good thermal conductivity at high temperatures [14, 15]. These properties, along with other mechanical properties such as high hardness and high compressive strength, make ZrB_2 very accommodative for applications that need to withstand high temperatures, such as space and aerospace applications [16–20].

Due to the high thermal conductivity coefficient of some ceramics, such as ZrB_2, their use in heat exchangers with ceramic walls has been considered. First, Tuckerman and Pease [21] investigated a micro heat exchanger made of silicon. The heat flux of this converter, which was 790 W/cm^2, showed the outstanding capability of this type of heat exchanger. Alm et al. [4] investigated the performance of a micro heat exchanger made of alumina to investigate the heat transfer rate in both counter-flow and cross-flow regimes. For mass flow rates of 20–120 kg/h, they reported that the efficiency ranged from 0.1 to 0.22.

Mello et al. [22] investigated the heat transfer and pressure drop in an experimentally made ceramic heat exchanger with plates and vanes. The heat exchanger showed very good performance at temperatures up to 890 °C and with Reynolds numbers between 200 and 500, so using ceramics to fabricate high-temperature heat exchangers is recognized as the best option. Fend et al. [23] tested SiC heat exchangers under high-temperature conditions. The test was carried out on two SiC heat exchangers with different thicknesses and dimensions at a temperature of up to 950 °C. The results indicated better performance of the sample with wider channels due to thinner walls. In general, the effectiveness of up to 65% and a heat transfer rate to volume ratio of 995 m^2/m^3 were reported for these heat exchangers.

Sommers et al. [12] conducted a comprehensive study on the applications of advanced ceramic materials and their advantages in air conditioning applications and reported the current status of ceramic materials for use in a variety of heat transfer systems. Fattahi et al. [24] investigated the effect of using AlN ceramics on the heat transfer performance of microchannel heat exchangers. They reported a 26% and 59% increase in the efficiency and heat transfer of micro heat exchangers, respectively, by substituting AlN for Al_2O. Lewinsohn et al. [25] scrutinized the microchannel heat exchanger using SiC plates and conducted studies on efficiency, temperature distribution, pressure drop, and thermal stress in both warm and cold plates, which led to better efficiency in microturbine cycles. Nekahi et al. [8] employed ultrahigh temperature ceramics instead of metals in micro heat exchangers. Through a numerical simulation, the thermal performance of the heat exchangers using TiB_2-SiC and TiB_2-SiC-C_f ceramics was investigated. Reports have shown the increase in heat transfer using TiB_2-SiC compared to Al_2O_3 and also the superiority of using TiB_2-SiC-C_f compared to Al_2O_3 at a specific mass flow rate of 20.4 kg/h.

In the current research, the goal is to improve the performance of a heat sink microchannel made of fully dense ZrB_2 ceramic using the Taguchi methodology. The impact of three fluid flow parameters (mass flow rate, gauge outlet pressure, and inlet temperature) on the performance of heat sink microchannels are studied. To optimize the performance, six output parameters (warm outlet temperature, cold outlet temperature, heat transfer, effectiveness, pressure drop in cold channel, and pressure drop in warm channel) are analyzed by ANOVA calculations.

Table 1. Selected quality characteristics for output parameters of heat sink microchannels.

Output parameter	Quality characteristic
Warm outlet temperature	"The-lower-the-better"
Cold outlet temperature	"The-higher-the-better"
Heat transfer	"The-higher-the-better"
Effectiveness	"The-higher-the-better"
Pressure drop in the cold channel	"The-lower-the-better"
Pressure drop in warm channel	"The-lower-the-better"

2. Methodology

2.1. Design of experiments

The Taguchi method is a design-of-experiments tool that employs orthogonal arrays to optimize the levels of investigated parameters. This methodology is planned not only to save time but also to enhance the generation of mathematical/statistical information from limited results. Such an approach assists in detecting the role/significance of some parameters affecting the process and discloses any possible correlations between input and output values. Using the Taguchi method helps determine the optimum investigating parameters to design and fabricate a system/product with better performance and higher quality or standard. This method categorizes quality characteristics into three classes: "the-nominal-the-better", "the-lower-the-better", or "the-higher-the-better" [26]. In the current research, the goal is to improve the performance of a heat sink microchannel made of fully dense ZrB_2 ceramic. Six output parameters (warm outlet temperature, cold outlet temperature, heat transfer, effectiveness, pressure drop in cold channel, and pressure drop in warm channel) are analyzed to achieve that goal. Therefore, the quality characteristics are selected based on the classes listed in Table 1.

Table 2. Fluid parameters and selected levels.

Parameter	Level 1	Level 2	Level 3
Mass flow rate (kg/h)	20	60	100
Gauge outlet pressure (bar)	0	1	2
Inlet temperature (°C)	10	30	50

Table 3. Numerical analysis procedure (L9 orthogonal array).

Run no.	Mass flow rate (kg/h)	Gauge outlet pressure (bar)	Inlet temperature (°C)
1	20	0	10
2	20	1	30
3	20	2	50
4	60	0	30
5	60	1	50
6	60	2	10
7	100	0	50
8	100	1	10
9	100	2	30

Additionally, performing analysis of variance (ANOVA) helps estimate the significance and contribution of all input parameters on the performance of output items. In this study, the researchers used the Qualitek-4 package (developed by Nutek Inc., USA) to design the experiments and conduct the statistical analyses. The significance and contribution of three fluid parameters (mass flow rate, gauge outlet pressure, and inlet temperature) on the performance of ZrB_2 heat sink microchannels are determined. The input parameters are studied at three levels (listed in Table 2). While a traditional full factorial design requires 27 runs, the Taguchi methodology enables us to perform only 9 runs by employing an L9 orthogonal array option, listed in Table 3.

2.2. Geometry of the micro heat exchanger

In the present study, a micro heat exchanger made of zirconium diboride is investigated numerically as a benchmark. The chosen micro heat exchanger is designed to operate with water as the warm and cold fluids. A schematic of the heat exchanger is demonstrated in Fig. 1. The plates of the heat exchanger are made of ZrB_2, which contain microchannels. Table 4 provides the geometrical data of the plates and channels of the heat exchanger. Due to the periodic nature of the heat exchanger microchannels, the whole geometry is not investigated numerically, and an element of the channels, shown in Fig. 1, is used to study the heat transfer.

Table 4. Geometrical data of the pale micro heat exchanger.

	Warm water	Cold water
Number of plates	3	3
Number of channels	17	17
Total number of channels	51	51
Channel length (mm)	12.5	12.5
Channel width (μm)	250	250
Channel height (μm)	320	420
Wall thickness (μm)	520	520
Layer thickness (μm)	990	880

2.3. Governing equations and the numerical procedure

Heat transfer in a heat exchanger consists of two mechanisms: heat conduction in the ZrB_2 made plates and the heat convection in the fluids. Therefore, three domains are defined to model the heat transfer: two fluid domains for cold and warm water, and a solid domain for plates.

The governing equations for the fluid domains are continuity, Navier-stokes, and energy equation, which are as follows [11, 27, 28]:

$$\rho\nabla.(u) = 0 \tag{1}$$

$$\rho\left(\frac{\partial u}{\partial t} + u.\nabla u\right) = -\nabla p + \nabla.\left(\mu(\nabla u + (\nabla u)^T - \frac{2}{3}\mu(\nabla u)I\right) \tag{2}$$

$$\rho c_p u.\nabla T + \nabla.q = Q \tag{3}$$

where u, ρ, μ, c_p, T, and q stand for velocity (m/s), fluid viscosity (Pa.s), heat capacity (J/kg.K), temperature (K), and heat flux (W/m^2), respectively. Q represents the heat generation in the fluid, which is ignored in the current study. Heat flux (q) is calculated using Fourier's law for heat conduction as [28]:

$$q = -k\nabla T \tag{4}$$

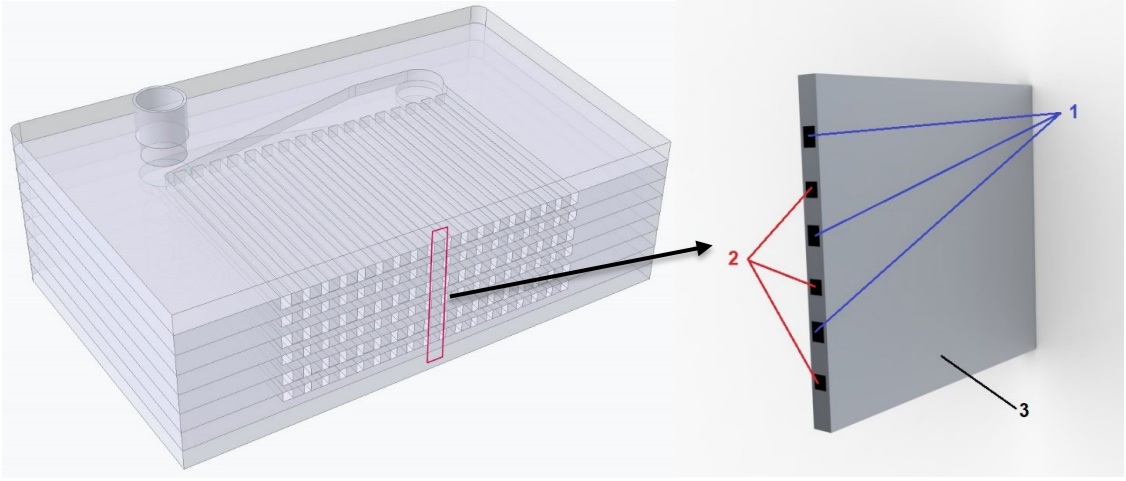

Fig. 1. Geometry of the micro heat exchanger (1: cold flow passages, 2: warm flow passages, 3: solid ceramic body).

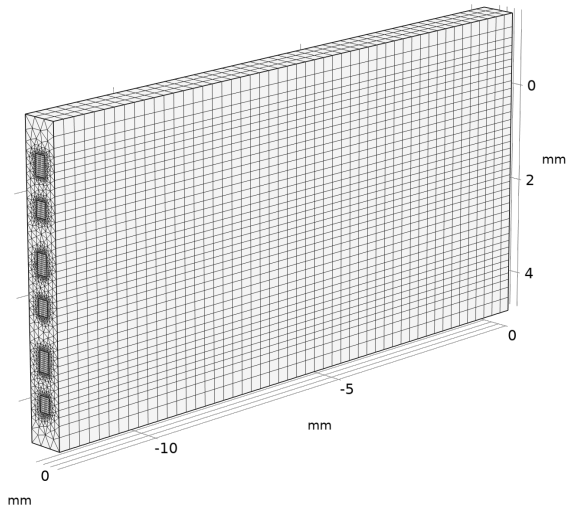

Fig. 2. Meshed computational domain.

It should be noted that k (W/m.K) is the materials heat transfer coefficient.

On the other hand, the governing equation for the solid domain is the steady-state 3D heat conduction equation as follows [8]:

$$\nabla.q = Q \tag{5}$$

Conjugate heat transfer is used to relate the abovementioned equations for solid and fluid domains. The equations are solved numerically using COMSOL Multiphysics software and the results are obtained as velocity and temperature distribution in the fluid and solid domains.

To solve the governing equations, the solid and fluid domains are meshed as represented in Fig. 2. The number of elements can affect the convergence and the results. Therefore, the mesh independency check is done, and the least number of elements is 29740 to get reliable results.

An important parameter in the heat exchanger performance evaluation is effectiveness (ε), which is defined as the actual heat transfer to the maximum possible heat transfer in the heat exchanger. In the current study ε is used based on the inlet and outlet temperatures of the fluids [29]:

$$\varepsilon = \frac{T_{wo} - T_{wi}}{T_{ci} - T_{wi}} \tag{6}$$

where c and w subscripts represent the cold and warm fluids, respectively, while *o* and *i* stand for outlet and inlet, respectively.

3. Results and discussion

The heat transfer is analyzed in the ZrB_2-made micro heat exchanger by COMSOL Multiphysics and temperature distribution in both fluid domains and the solid domain are obtained. These results would be used for the optimization process to find out the essential parameters effective on the heat exchanger performance. First, the numerical data is compared with the results of Alm et al. [4] to make sure about the data. Fig. 3 demonstrates the difference between the numerical results of the present work and the reference data that confirms the correctness of the applied numerical method.

Fig. 4 shows the temperature distribution in the whole heat exchanger made of ZrB_2. The contours are shown for all 9 cases proposed

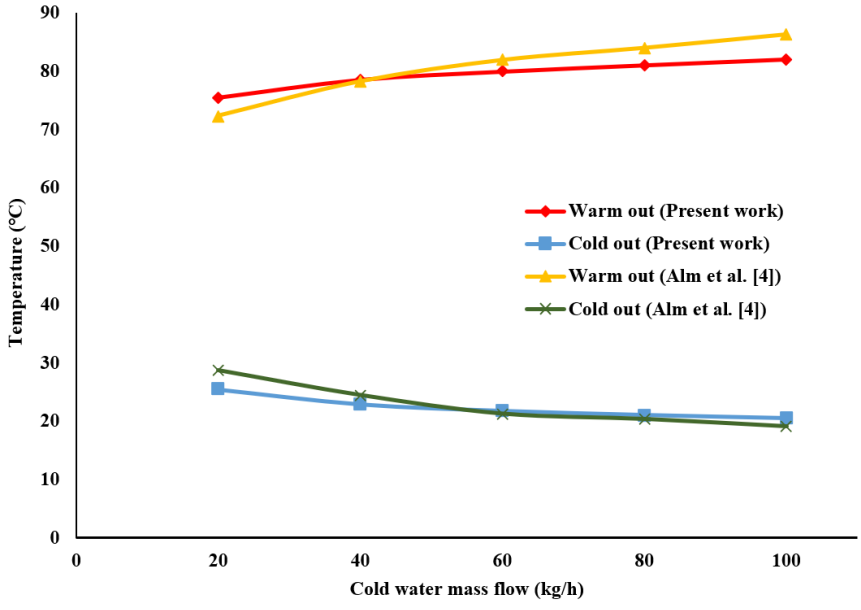

Fig. 3. The comparison of the fluids outlet temperature with the results of Alm et al. [4].

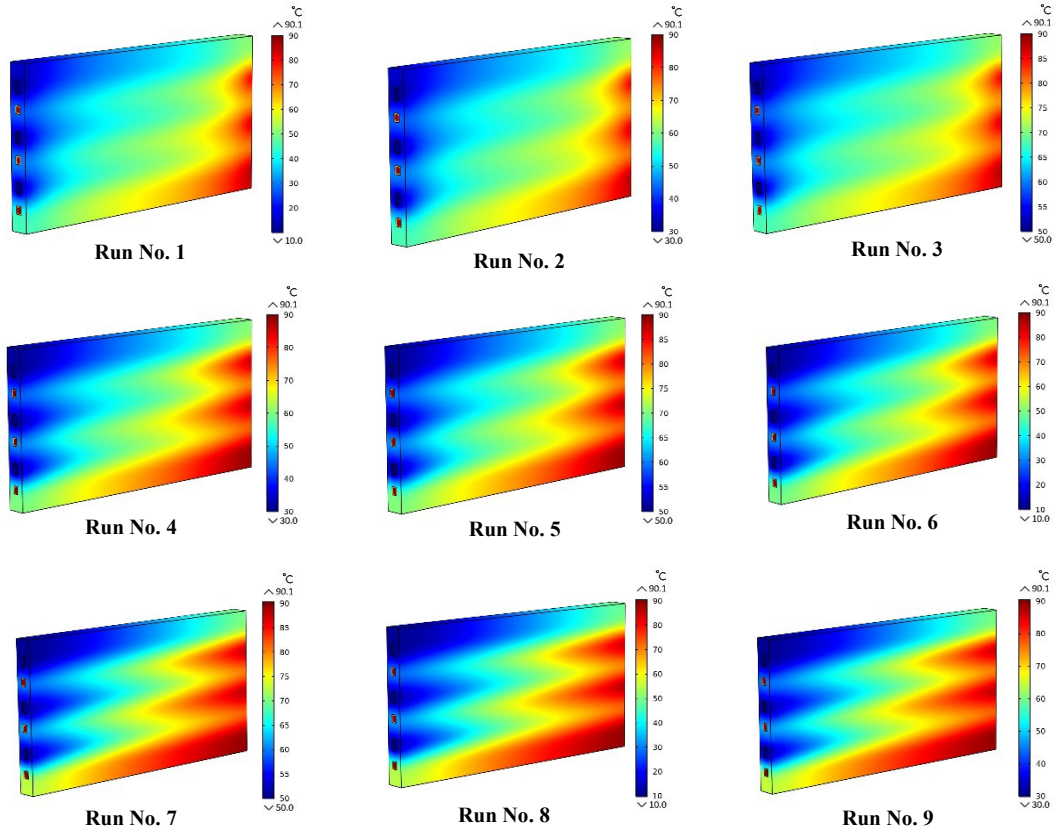

Fig. 4. Temperature contours for ZrB_2-made micro heat exchanger in different cases.

in Table 3. These data are used as the input parameters of the optimization algorithm. Then, the results of the output parameters, including warm outlet temperature, cold outlet temperature, heat transfer, effectiveness, pressure drop in the cold channel, and pressure drop in the warm channel, are listed in Table 5. Moreover, the grand averages of the results and their standard deviations are also calculated and inserted in this table. As previously presented in Table 1, it is desirable that the warm outlet

Table 5. Numerical results of the output parameters.

Run No.	Warm outlet temp. (°C)	Cold outlet temp. (°C)	Heat transfers (J/s)	Effectiveness (%)	Pressure drop in the cold channel (Pa)	Pressure drop in the warm channel (Pa)
1	70.60	27.04	520.21	24.30	9926	7841
2	75.66	43.17	389.64	23.97	6817	7061
3	80.53	58.95	260.11	23.76	5225	6425
4	79.04	40.35	645.83	18.34	17931	20349
5	82.77	57.02	430.11	18.19	13963	18629
6	75.20	23.46	873.50	18.56	26690	22617
7	83.50	56.40	582.90	16.37	22268	30181
8	76.74	22.55	1193.70	16.63	39380	36164
9	80.23	39.65	882.98	16.30	27558	32965
Grand average	78.25	40.95	642.11	19.60	18862	20248
Standard deviation	4.10	14.43	293.43	3.41	11210	11406

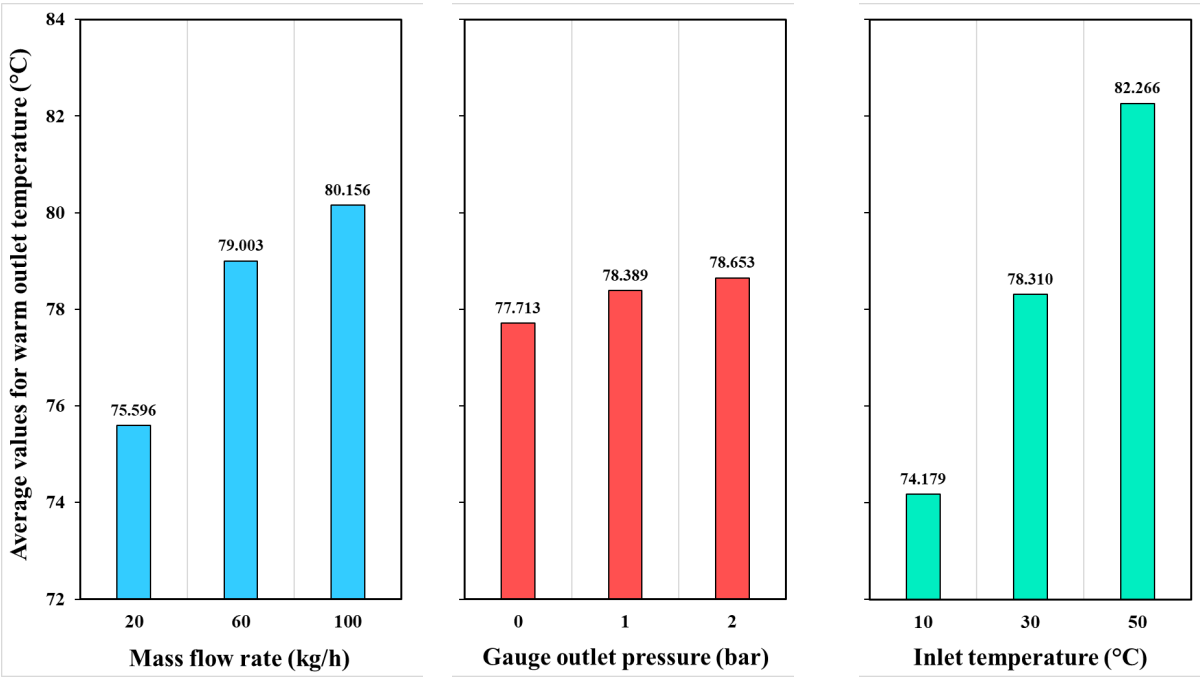

Fig. 5. Main effect plots of the average values for warm outlet temperature.

temperature and the pressure drop in both warm and cold channels should be as low as possible, but the cold outlet temperature, heat transfer, and effectiveness should be as high as possible. Therefore, among the 9 runs, Run No. 1 has the best performance in terms of warm outlet temperature and effectiveness. Run No. 3 provides the best results from the viewpoints of cold outlet temperature and pressure drop in both cold and warm channels. The interesting thing is that the lowest heat transfer is achieved for this run. The implementation of Run No. 8 causes the highest heat transfer, while it results in the weakest result from the point of view of pressure drop in both cold and warm channels. It seems that the best condition for heat transfer is the worst case for pressure drop in both cold and warm channels and vice versa.

3.1. Warm outlet temperature

Fig. 5 shows the main effects plots showing the average values for warm outlet temperature. As it can be seen, with the increase in the mass flow rate from 20 to 60 kg/h, the average value of warm outlet temperature increases remarkably, but with a further increase in the mass flow rate to 100 kg/h, the average value experiences a smaller increase. Although the average values for warm outlet temperature increase with the increase of gauge outlet pressure from 0 to 1 bar and then to 2 bar, the intensity of the changes is very small and cannot be compared with the mass flow rate variations. According to the trend of extreme changes in the average values for warm outlet temperature with the increase of inlet temperature from 10 to 30 °C and then to 50 °C, it seems that the warm outlet temperature is very sensitive to the inlet temperature. Since it is better to have a lower warm outlet temperature for better heat exchanger performance, it seems that a mass flow rate of 20 kg/h, a gauge outlet pressure of 0 bar, and an inlet temperature of 10 °C are the best conditions in this regard.

Table 6. ANOVA results of the significance of fluid parameters on warm outlet temperature.

Parameter	Degrees of freedom	Sum of squares	Variance	F-ratio	Pure sum	Significance (%)
Mass flow rate	2	33.733	16.866	25.824	32.427	24.100
Gauge outlet pressure	2	1.404	0.702	1.075	0.098	0.073
Inlet temperature	2	98.103	49.051	75.102	96.797	71.942
Other/error	2	1.305	0.652	-	-	3.885
Total	8	134.548	-	-	-	100.000

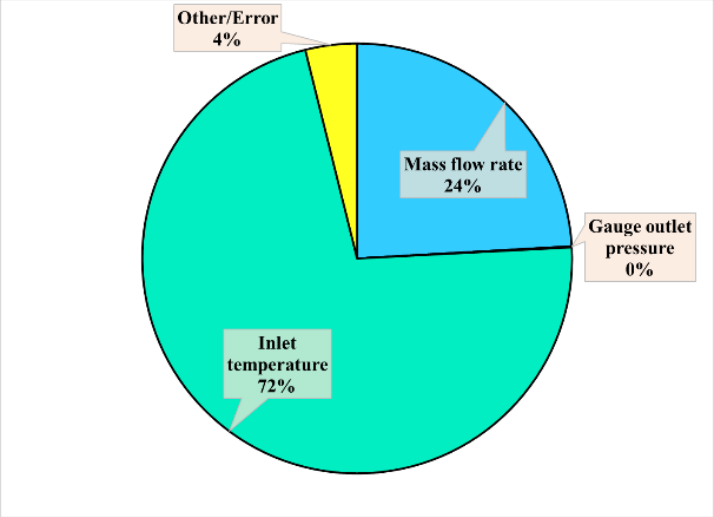

Fig. 6. Pie chart of significant fluid parameters on warm outlet temperature.

The analysis of the variance of the significance of fluid parameters (mass flow rate, gauge outlet pressure, and inlet temperature) on the warm outlet temperature is presented in Table 6. According to these statistical calculations, the inlet temperature is recognized as the main fluid parameter controlling the warm outlet temperature with the highest significance of ~72%. The significance of the mass flow rate is about 24% and gauge outlet pressure is almost insignificant according to ANOVA. The significance of other unstudied parameters and/or errors is around 4%, which is almost negligible.

A better perspective of the data regarding the significance of investigated fluid parameters is provided in a pie chart (Fig. 6). As expected, no effect of the gauge outlet pressure is seen in the figure as it is an insignificant parameter. Errors and unknown parameters are less than 4%, which can be ignored from a statistical point of view in this research. Hence, according to the defined parameters and designed levels in the methodology section, it appears that inlet temperature and mass flow rate have considerable importance on warm outlet temperature. It is completely in accordance with the heat transfer phenomena: the higher the temperature difference (lower cold inlet temperature), the higher heat transfer means a lower warm outlet.

The optimal conditions and the contribution of fluid parameters on warm outlet temperature are presented in Table 7. The lowest warm outlet temperature can be accessible at the optimum conditions, i.e., the mass flow rate of 20 kg/h (level 1), the gauge outlet pressure of 0 bar (level 1), and the inlet temperature of 10 °C (level 1). The contributions of mass flow rate, gauge outlet pressure, and inlet temperature are calculated as -2.66, -0.54, and -4.07 °C, respectively. Therefore, total contributions from all fluid parameters are -7.27 °C. Based on the results reported in Table 5, the grand average of warm outlet temperature is 78.25 °C, which can be decreased by selecting the optimized fluid parameters. Considering the contribution of all fluid parameters under optimal conditions (-7.27 °C), the warm outlet temperature is expected to drop to 70.98 °C. It should be noted that this optimal condition (all parameters at level 1) is, by chance, exactly the same as the condition of Run No. 1. The numerical result of the warm outlet temperature for Run No. 1 is 70.60 °C (Table 5), which is very close to the expected outcome based on statistical calculations in Table 7 (70.98 °C).

Table 7. Contribution of fluid parameters on warm outlet temperature.

Parameter	Level	Level description	Contribution (°C)
Mass flow rate (kg/h)	1	20	-2.66
Gauge outlet pressure (bar)	1	0	-0.54
Inlet temperature (°C)	1	10	-4.07
Total contributions from all parameters			-7.27
Current grand average of warm outlet temperature			78.25
The expected result at optimum conditions			70.98

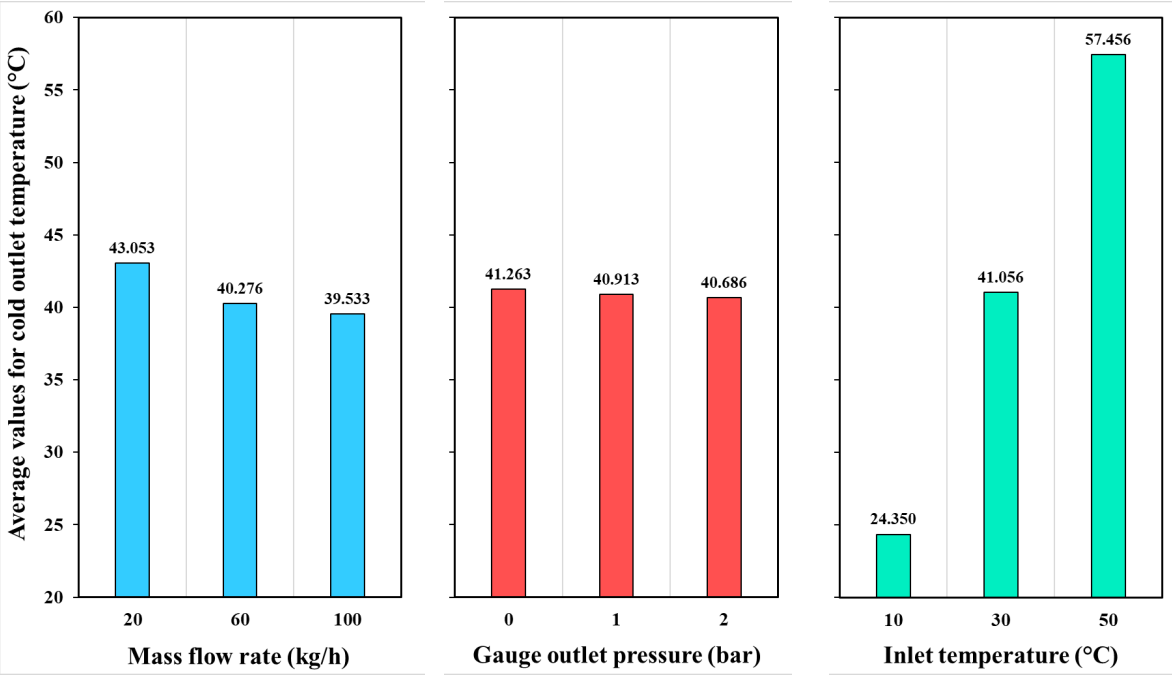

Fig. 7. Main effect plots of the average values for cold outlet temperature.

3.2. Cold outlet temperature

The main effects plots showing the average values for cold outlet temperature are illustrated in Fig. 7. With increasing the mass flow rate from 20 to 60 kg/h, the average value of cold outlet temperature decreases by about 3 °C, and with more increase in the mass flow rate to 100 kg/h, the average value slightly drops (less than 1 °C). The average values of cold outlet temperature decrease negligibly as the gauge outlet pressure increases from 0 to 1 bar and then to 2 bar, but the amount of this drop is so small that it can be ignored. Although cold outlet temperature does not show much sensitivity to mass flow rate and gauge outlet pressure, this parameter is very sensitive to inlet temperature increasing from 10 to 30 °C and then to 50 ° C. Since it is desirable to have a higher cold outlet temperature for better performance of heat exchangers, it appears that a mass flow rate of 20 kg/h, a gauge outlet pressure of 0 bar, and an inlet temperature of 50 °C are the best fluid conditions.

Table 8 presents the analysis of the variance of the significance of fluid parameters (mass flow rate, gauge outlet pressure, and inlet temperature) on the cold outlet temperature. Based on these statistical computations, the inlet temperature is identified as the main and the only influential parameter controlling the cold outlet temperature with a giant significance of ~99%. According to ANOVA, the significance of the mass flow rate is around 1%, and gauge outlet pressure is completely insignificant. The significance of the errors and other unstudied parameters is also ignorable. Therefore, the inlet temperature can be considered as the only factor affecting the cold outlet temperature.

Table 8. ANOVA results of the significance of fluid parameters on cold outlet temperature.

Parameter	Degrees of freedom	Sum of squares	Variance	F-ratio	Pure sum	Significance (%)
Mass flow rate	2	20.652	10.326	34.928	20.060	1.204
Gauge outlet pressure	2	0.506	0.253	0.857	0.000	0.000
Inlet temperature	2	1644.123	822.061	2780.697	1643.532	98.658
Other/error	2	0.59	0.295	-	-	0.138
Total	8	1665.873	-	-	-	100.000

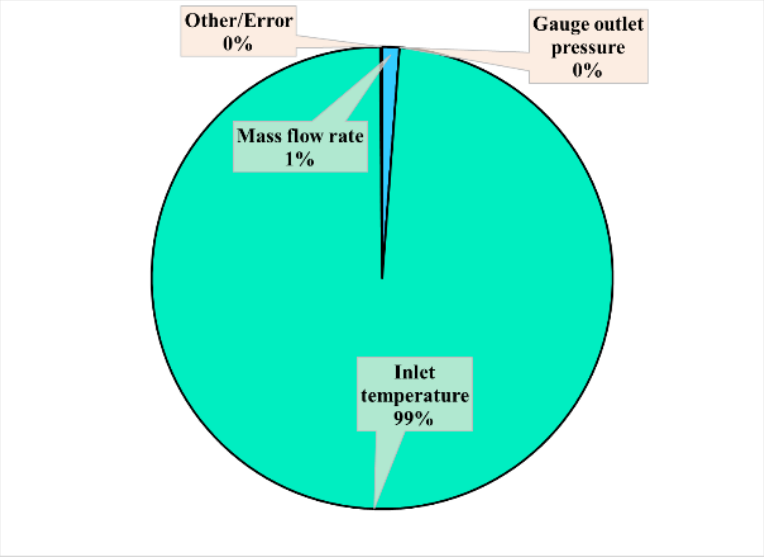

Fig. 8. Pie chart of significant fluid parameters on cold outlet temperature.

The pie chart of significant fluid parameters on cold outlet temperature is shown in Fig. 8, which clearly verifies that only inlet temperature is very significant and other studied and unstudied parameters, as well as errors, are not significant. In other words, it can be understood from this chart that in the range of parameters and levels designed in this research, only the control of the inlet temperature is important, and other parameters do not need to be controlled, from the point of view of cold outlet temperature.

Table 9 lists the optimum conditions and fluid parameters' contribution to cold outlet temperature. The highest cold outlet temperature can be obtained at the optimal conditions: the mass flow rate of 20 kg/h (level 1), the gauge outlet pressure of 0 bar (level 1), and the inlet temperature of 50 °C (level 3). The contributions of mass flow rate, gauge outlet pressure, and inlet temperature are computed as 2.10, 0.31, and 16.50 °C, respectively. Hence, the total contributions from all fluid parameters are 18.91 °C. On the basis of the results summarized in Table 5, the grand average of cold outlet temperature is 40.95 °C, which can be enhanced by choosing the optimized fluid parameters. Therefore, the cold outlet temperature is expected to increase to 59.86 °C under optimal conditions by considering the contribution of all fluid parameters.

Table 9. Contribution of fluid parameters on cold outlet temperature.

Parameter	Level	Level description	Contribution (°C)
Mass flow rate (kg/h)	1	20	2.10
Gauge outlet pressure (bar)	1	0	0.31
Inlet temperature (°C)	3	50	16.50
Total contributions from all parameters			18.91
Current grand average of cold outlet temperature			40.95
The expected result at optimum conditions			59.86

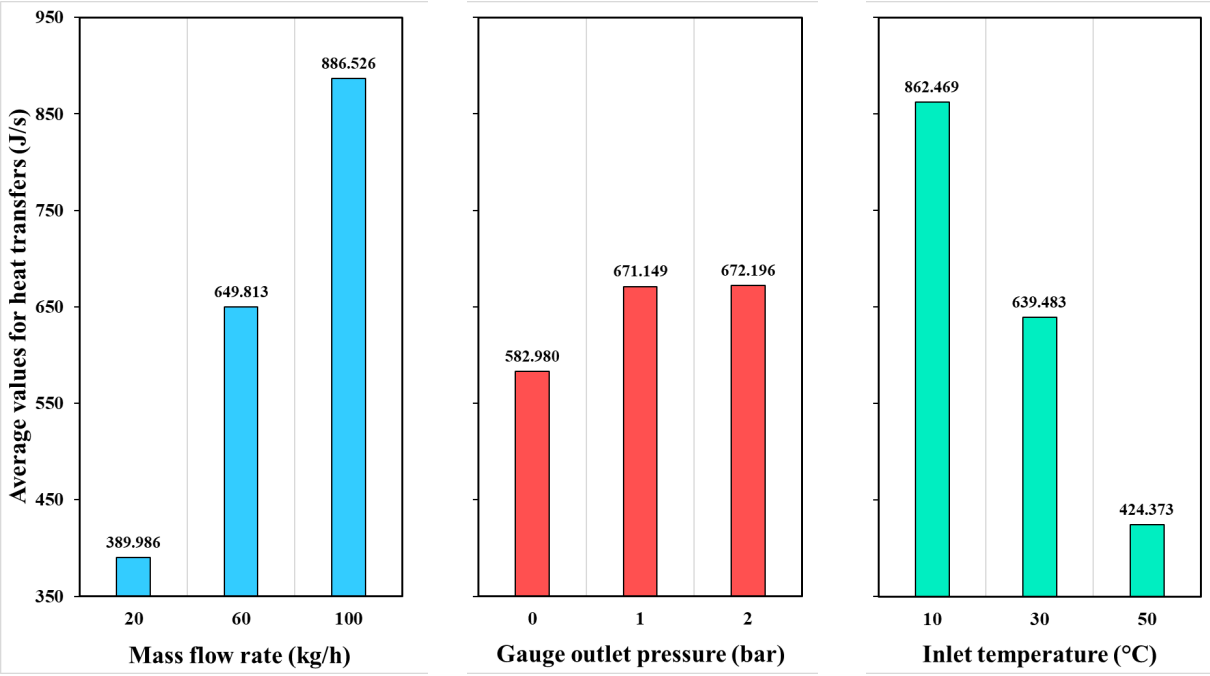

Fig. 9. Main effect plots of the average values for heat transfer.

3.3. Heat transfer

One of the most important factors affecting the performance of a heat exchanger is its heat transfer ability. The main effects plots illustrating the average values for heat transfer are given in Fig. 9. With increasing the mass flow rate from 20 to 60 kg/h, the average value of heat transfer enhances sharply from ~390 to ~650 J/s. As the mass flow rate is further increased to 100 kg/h, the average value increases significantly to ~887 J/s. Contrary to the observations of the insignificant effect of changes in gauge outlet pressure on warm and cold outlet temperatures, with the increase of gauge outlet pressure from 0 to 1 bar, the average values for heat transfer increase from ~583 to ~671 J/s. However, a further increase of gauge outlet pressure up to 2 bar does not have another tangible effect. The effect of changing the inlet temperature on the average values for heat transfer, like the mass flow rate, is very great, but the trend is completely opposite. In other words, with the increase of the inlet temperature from 10 to 30 °C and then to 50 °C, the average values for heat transfer dropped drastically. For better performance of a heat exchanger, more heat transfer is suitable. Hence, a mass flow rate of 100 kg/h, a gauge outlet pressure of 2 bar (the same result is almost obtainable with 1 bar), and an inlet temperature of 10 °C are the best fluid conditions.

The significant results of the analysis of the variance of fluid parameters (mass flow rate, gauge outlet pressure, and inlet temperature) on the heat transfer are provided in Table 10. Mass flow rate is discovered as the main fluid parameter controlling the heat transfer, according to the statistical approach, with a significance of ~51%. On the basis of ANOVA, the significance of inlet temperature is also considerable with a value of ~40%. Despite the visible effect of increasing the gauge outlet pressure from 0 to 1 bar on the average values for heat transfer in Fig. 9, the analysis of variance again estimates this parameter to be insignificant. Moreover, the significance of the errors and/or unknown parameters is around 9%.

Table 10. ANOVA results of the significance of fluid parameters on heat transfer.

Parameter	Degrees of freedom	Sum of squares	Variance	F-ratio	Pure sum	Significance (%)
Mass flow rate	2	370094.963	185047.481	24.597	355048.947	51.546
Gauge outlet pressure	2	15734.634	7867.317	1.045	688.618	0.099
Inlet temperature	2	287923.913	143961.956	19.136	272877.897	39.616
Other/error	2	15046.016	7523.008	-	-	8.739
Total	8	688799.529	-	-	-	100.000

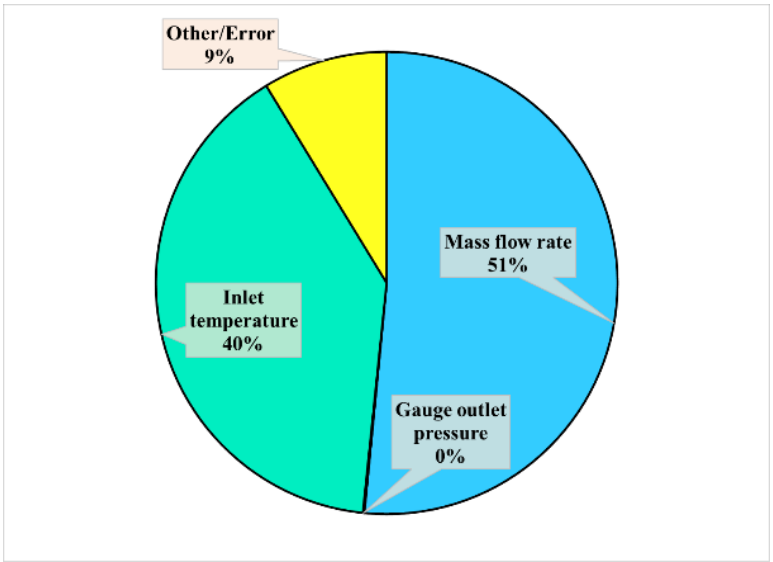

Fig. 10. Pie chart of significant fluid parameters on heat transfer.

Fig. 10 is a pie chart showing the importance of fluid parameters in heat transfer, which obviously shows the significance of mass flow rate and inlet temperature. In other words, from the view of the heat exchanger's performance to cool the warm fluid more, both mass flow rate and cold fluid inlet temperature have almost the same significance. Although gauge outlet pressure is insignificant, other studied/unstudied parameters and errors are not. It can be concluded that, from the viewpoint of heat transfer in the range of designed parameters and levels in this study, it is essential to control the mass flow rate and inlet temperature. However, despite the control of both parameters, the significance of errors and unknown parameters is also remarkable.

The optimum conditions and the contribution of fluid parameters on heat transfer are summarized in Table 11. More heat transfer can be achieved at the optimal conditions: the mass flow rate of 100 kg/h (level 3), the gauge outlet pressure of 2 bar (level 3), and the inlet temperature of 10 °C (level 1). The contributions of mass flow rate, gauge outlet pressure, and inlet temperature are calculated as 244.42, 30.09, and 220.36 J/s, respectively. Thus, total contributions from all fluid parameters are 494.87 J/s. In accordance with the results reported in Table 5, the grand average of heat transfer is 642.11 J/s, which can be boosted via the selection of the optimal fluid parameters. Hence, by considering the contribution of all fluid parameters, the heat transfer is expected to reach 1136.98 J/s under optimum conditions.

Table 11. Contribution of fluid parameters on heat transfer.

Parameter	Level	Level description	Contribution (J/s)
Mass flow rate (kg/h)	3	100	244.42
Gauge outlet pressure (bar)	3	2	30.09
Inlet temperature (°C)	1	10	220.36
Total contributions from all parameters			494.87
Current grand average of heat transfer			642.11
Expected result at optimum conditions			1136.98

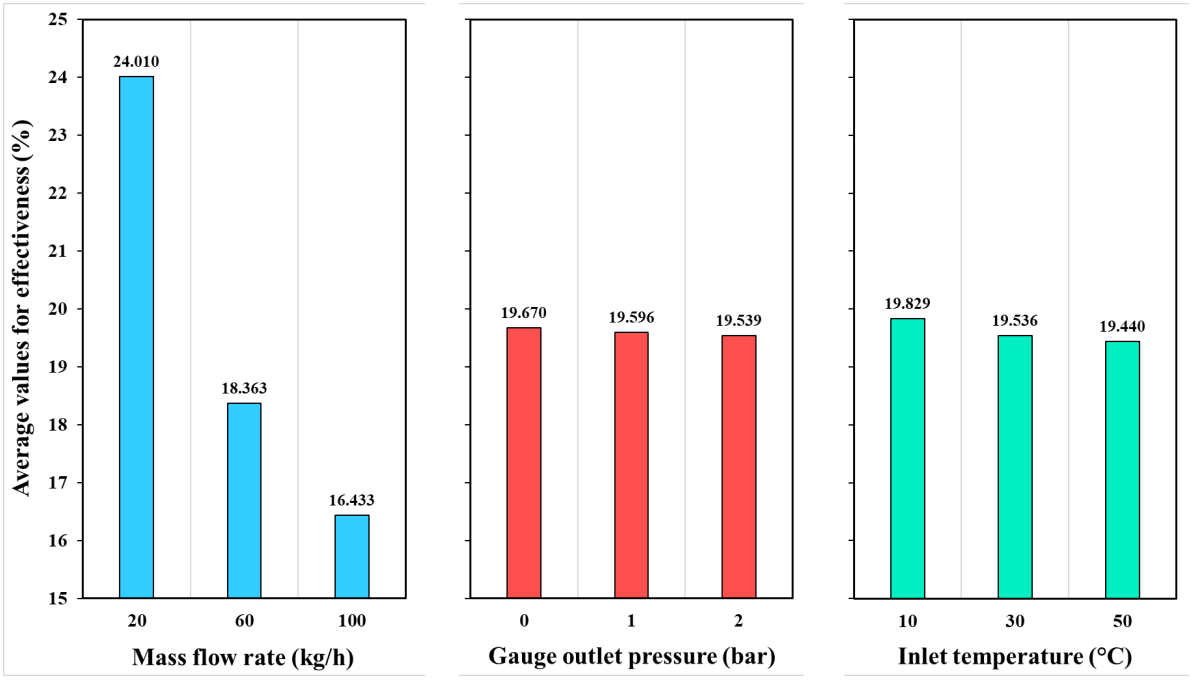

Fig. 11. Main effect plots of the average values for effectiveness.

3.4. Effectiveness

Fig. 11 depicts the main effects plots presenting the average values for effectiveness. The average value of effectiveness decreases sharply from ~24% to ~18% with increasing the mass flow rate from 20 to 60 kg/h. The average value decreases with a lower drop rate to ~16% as the mass flow rate is further increased to 100 kg/h. The average values for effectiveness show a very small decrease with changes in gauge outlet pressure, a trend similar to the cases analyzed before. A different outcome compared to the previous cases is observed in the investigation of the effect of the inlet temperature on the average values for effectiveness, where, similar to the gauge outlet pressure, its changes do not have much effect on the effectiveness. By increasing the gauge outlet pressure from 0 to 1 bar and then by 2 bar, as well as, by increasing the inlet temperature from 10 to 30 °C and then to 50 °C, the drop in the average values for effectiveness is so negligible that it can be considered constant at around 19%. Generally, higher effectiveness is desired for better performance of heat exchangers. Thus, a mass flow rate of 20 kg/h, a gauge outlet pressure of 0 bar, and an inlet temperature of 10 °C are the best fluid conditions. However, it should be noted that the same result may be almost obtainable with gauge outlet pressures of 1 or 2 bar and inlet temperatures of 30 or 50 °C.

Table 12 presents the analysis of the variance of fluid parameters (mass flow rate, gauge outlet pressure, and inlet temperature) significance on the effectiveness. Mass flow rate is identified as the main and only controlling parameter, with a significance of ~100%, based on statistical computations. According to ANOVA, the significances of inlet temperature and gauge outlet pressure are about zero. Interestingly, the significance of errors and unknown parameters is also around zero. These calculations are consistent with the plots in Fig. 11, which shows that parameters other than mass flow rate are insignificant.

Table 12. ANOVA results of significance of fluid parameters on effectiveness.

Parameter	Degrees of freedom	Sum of squares	Variance	F-ratio	Pure sum	Significance (%)
Mass flow rate	2	93.015	46.507	18080.021	93.010	99.696
Gauge outlet pressure	2	0.025	0.012	4.939	0.020	0.021
Inlet temperature	2	0.247	0.123	48.091	0.242	0.259
Other/error	2	0.004	0.002	-	-	0.024
Total	8	93.293	-	-	-	100.000

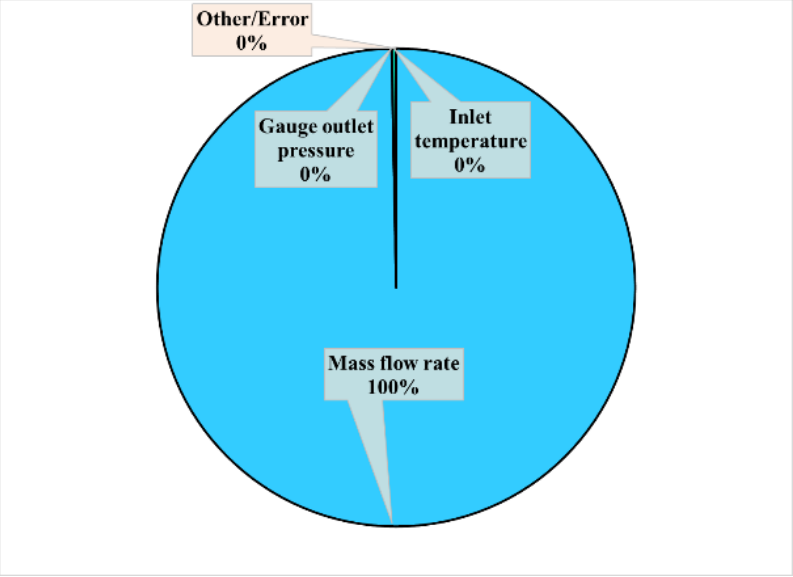

Fig. 12. Pie chart of significant fluid parameters on effectiveness.

The pie chart of significant fluid parameters on effectiveness, shown in Fig. 12, also illustrates the fact that the only influential parameter on effectiveness is mass flow rate, and other items such as errors and studied/unstudied parameters are unimportant. Thus, from the viewpoint of effectiveness in the range of investigated parameters and levels in this research, it is enough to control the mass flow rate and there is no need to control other parameters. This result shows the effectiveness, as introduced in Eq. 6, completely relies on the mass flow rate of the fluids and cannot be enhanced by means of an increase in temperature difference.

Table 13 summarizes the optimum conditions and the contribution of fluid parameters on effectiveness. Greater effectiveness can be approached at the optimal conditions: the mass flow rate of 20 kg/h (level 1), the gauge outlet pressure of 0 bar (level 1), and the inlet temperature of 10 °C (level 1). The contributions of mass flow rate, gauge outlet pressure, and inlet temperature are estimated as 4.40, 0.07, and 0.23%, respectively. Hence, total contributions from all fluid parameters are 4.70%. According to the results listed in Table 5, the grand average of effectiveness is 19.60% that can be extra-enhanced through choosing the optimal fluid parameters. Therefore, by considering the contribution of all fluid parameters, under optimum conditions, the effectiveness is expected to approach 24.30%. Again, it should be mentioned that such optimal condition (all parameters at level 1) is totally the same as the condition of Run No. 1. The numerical result of the effectiveness for Run No. 1 is 24.30 (Table 5), which is completely equal to the expected outcome based on statistical calculations in Table 13.

Table 13. Contribution of fluid parameters on effectiveness.

Parameter	Level	Level description	Contribution (%)
Mass flow rate (kg/h)	1	20	4.40
Gauge outlet pressure (bar)	1	0	0.07
Inlet temperature (°C)	1	10	0.23
Total contributions from all parameters			4.70
Current grand average of effectiveness			19.60
Expected result at optimum conditions			24.30

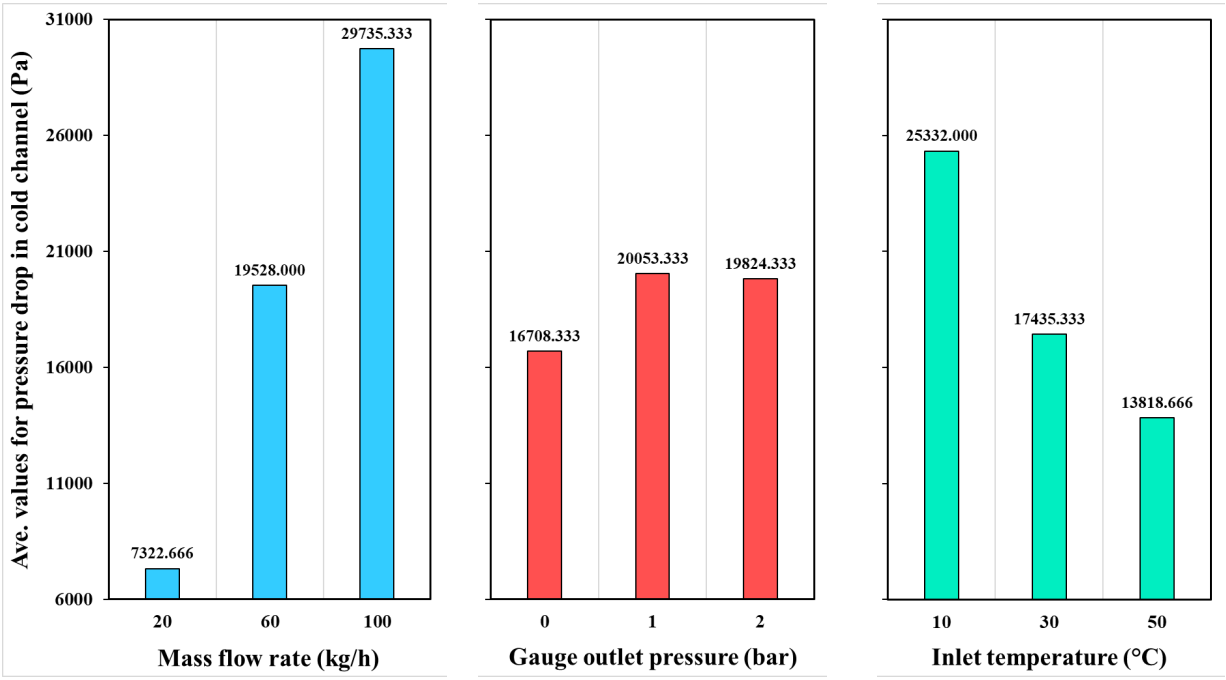

Fig. 13. Main effect plots of the average values for pressure drop in the cold channel.

3.5. Pressure drop in the cold channel

The main effects plots displaying the average values for pressure drop in the cold channel are shown in Fig. 13. The average value of pressure drop in the cold channel greatly increases from ~7300 to ~19500 Pa with increasing the mass flow rate from 20 to 60 kg/h. As the mass flow rate is further increased to 100 kg/h, the average value enhances again to ~29700 Pa. By increasing the gauge outlet pressure from 0 to 1 bar, the average value for pressure drop in the cold channel increases from ~16700 to ~20000 Pa, but with a further increase in gauge outlet pressure by 2 bar, a very slight drop to 19800 Pa is seen in the average value. The inlet temperature shows a behavior different from that of the mass flow rate, so that with the increase of the inlet temperature from 10 to 30 °C, the average value for pressure drop in cold channel decreases from ~25300 to ~17400 Pa, and the further increase of the inlet temperature to 50 °C causes the average value to drop to 13800 Pa. In fact, a lower pressure drop in the cold channel is appropriate for the better performance of a heat exchanger. Therefore, a mass flow rate of 20 kg/h, a gauge outlet pressure of 0 bar, and an inlet temperature of 50 °C are the best fluid conditions.

The analysis of the variance of the significance of fluid parameters (mass flow rate, gauge outlet pressure, and inlet temperature) on the pressure drop in the cold channel is provided in Table 14. Mass flow rate is recognized as the main controlling parameter, with a significance of ~73%, on the basis of the statistical calculations. In accordance with ANOVA, the significance of inlet temperature is about 19%. Similar to most of the previous cases, the significance of gauge outlet pressure is around zero. Additionally, with a significance of ~8%, errors and/or other unstudied parameters are not ignorable.

Table 14. ANOVA results of the significance of fluid parameters on pressure drop in the cold channel.

Parameter	Degrees of freedom	Sum of squares	Variance	F-ratio	Pure sum	Significance (%)
Mass flow rate	2	755487551.669	377743775.834	36.281	734664796.140	73.082
Gauge outlet pressure	2	20951143.039	10475571.519	1.006	128387.510	0.012
Inlet temperature	2	207994561.763	103997280.881	9.988	187171806.234	18.619
Other/error	2	20822755.528	10411377.764	-	-	8.287
Total	8	1005256012	-	-	-	100.000

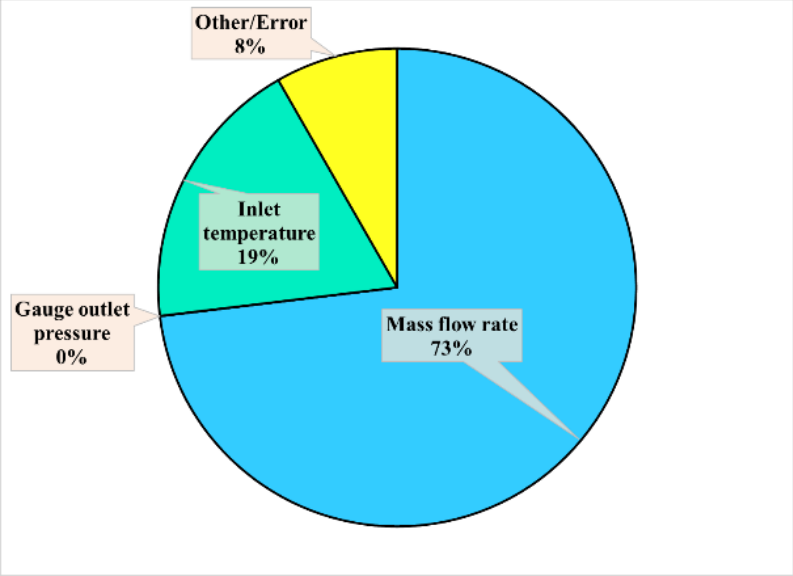

Fig. 14. Pie chart of significant fluid parameters on pressure drop in the cold channel.

Fig. 14 illustrates the pie chart of significant fluid parameters on pressure drop in the cold channel. This figure discloses that the main influential parameters on pressure drop in cold channels are mass flow rate and inlet temperature. Hence, from the viewpoint of pressure drop in the cold channel in the range of studied parameters and levels in this work, both mass flow rate and inlet temperature parameters must be controlled and monitored. With all these interpretations, the 8% significance of errors and other parameters cannot be ignored.

Table 15 presents the optimum conditions and the contribution of fluid parameters on pressure drop in the cold channel. Lower pressure drop in the cold channel can be achieved at the optimal conditions: the mass flow rate of 20 kg/h (level 1), the gauge outlet pressure of 0 bar (level 1), and the inlet temperature of 50 °C (level 3). The contributions of mass flow rate, gauge outlet pressure, and inlet temperature are calculated as -11539.33, -2153.67, and -5043.33 Pa, respectively. Thus, total contributions from all fluid parameters are -18736.33 Pa. Based on the data in Table 5, the average pressure drop in the cold channel is 18862 Pa, which can be decreased by selecting the optimal fluid parameters. Hence, the pressure drop in the cold channel is expected to be 125.67 Pa. Of course, this result seems somewhat strange, and it is not possible to comment on its correctness with certainty, and it requires more detailed and complete investigations.

Table 15. Contribution of fluid parameters on pressure drop in the cold channel.

Parameter	Level	Level description	Contribution (Pa)
Mass flow rate (kg/h)	1	20	-11539.33
Gauge outlet pressure (bar)	1	0	-2153.67
Inlet temperature (°C)	3	50	-5043.33
Total contributions from all parameters			-18736.33
Current grand average of pressure drop in the cold channel			18862
The expected result at optimum conditions			125.67

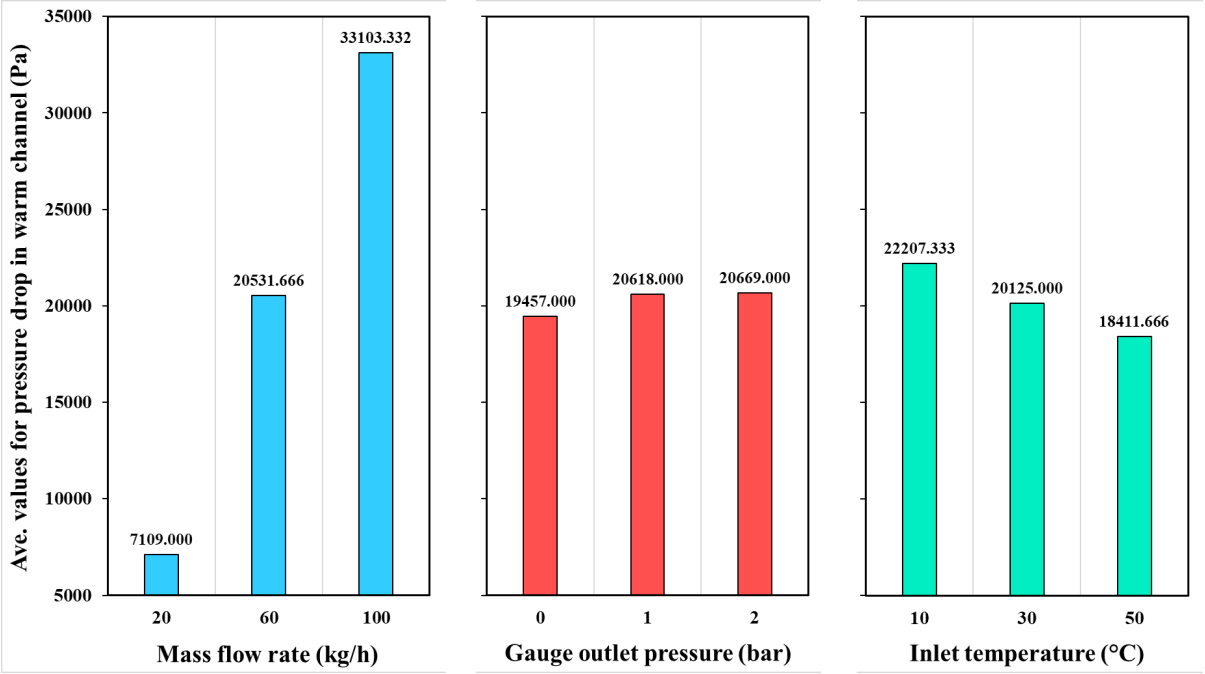

Fig. 15. Main effect plots of the average values for pressure drop in the warm channel.

3.6. Pressure drop in warm channel

Fig. 15 shows the main effects plots displaying the average values for pressure drop in warm channels. With increasing the mass flow rate from 20 to 60 kg/h, the average value of pressure drop in the warm channel sharply increases from ~7100 to ~20500 Pa. The average value intensifies more to ~33100 Pa as the mass flow rate is further increased to 100 kg/h. The average value for pressure drop in a warm channel increases from ~19400 to ~20600 Pa by increasing the gauge outlet pressure from 0 to 1 bar. With a further increase in gauge outlet pressure by 2 bar, a very slight enhancement in the average value is recorded. The inlet temperature presents a decreasing trend with the increase of the inlet temperature from 10 to 30 °C and then to 50 °C.

In general, a lower pressure drop in warm channels is desired for better performance of heat exchangers. Therefore, a mass flow rate of 20 kg/h, a gauge outlet pressure of 0 bar, and an inlet temperature of 50 °C are the best fluid conditions.

Table 16 summarizes the analysis of the variance of the significance of fluid parameters (mass flow rate, gauge outlet pressure, and inlet temperature) on the pressure drop in the warm channel. According to the statistical approach, the mass flow rate is identified as the main and dominant controlling parameter, with a significance of ~97%. Based on ANOVA, the significance of inlet

Table 16. ANOVA results of the significance of fluid parameters on pressure drop in the warm channel.

Parameter	Degrees of freedom	Sum of squares	Variance	F-ratio	Pure sum	Significance (%)
Mass flow rate	2	1013919809.845	506959904.922	416.034	1011482705.183	97.178
Gauge outlet pressure	2	2819466.000	1409733.000	1.156	382361.338	0.036
Inlet temperature	2	21678723.493	10839361.746	8.895	19241618.832	1.848
Other/error	2	2437104.661	1218552.330	-	-	0.938
Total	8	1040855104.000	-	-	-	100.000

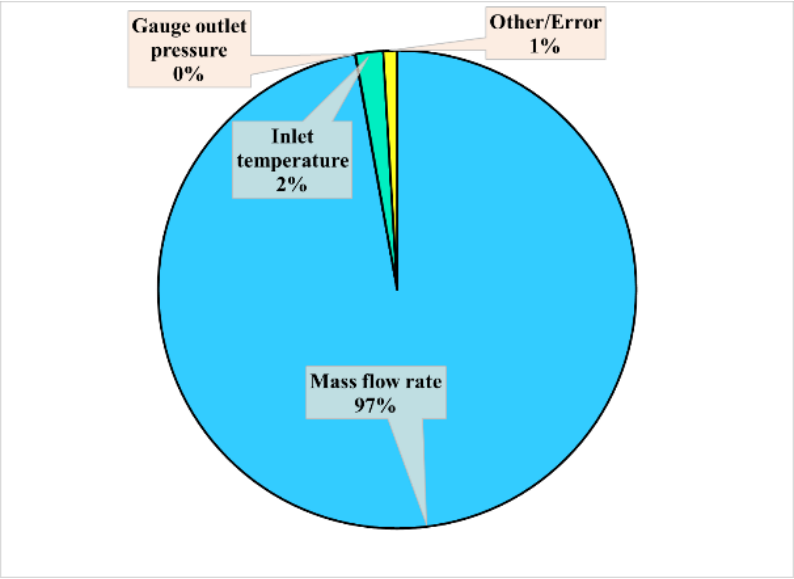

Fig. 16. Pie chart of significant fluid parameters on pressure drop in the warm channel.

temperature is very low (around 2%). As expected, the significance of gauge outlet pressure is also around zero. Finally, a significance of ~1% is recorded for errors and other parameters.

The pie chart of significant fluid parameters on pressure drop in the warm channel is displayed in Fig. 16, which illustrates that mass flow rate is the dominant controlling parameter on pressure drop in the warm channel. Therefore, only the mass flow rate must be monitored from the viewpoint of pressure drop in the warm channel in the range of studied parameters and levels in this research. Other parameters and errors are so insignificant that they can be neglected.

The optimum conditions and the contribution of fluid parameters on pressure drop in warm channels are listed in Table 17. Similar to pressure drop in a cold channel, lower pressure drop in a warm channel can be obtained at the optimal conditions: the mass flow rate of 20 kg/h (level 1), the gauge outlet pressure of 0 bar (level 1), and the inlet temperature of 50 °C (level 3). The contributions of mass flow rate, gauge outlet pressure, and inlet temperature are computed as -13139.00, -791.00, and -1836.33 Pa, respectively. Hence, total contributions from all fluid parameters are -15766.33 Pa. On the basis of the results reported in Table 5, the grand average of pressure drop in the warm channel is 20248 Pa, which can be dropped by choosing the optimal fluid parameters. Thus, the pressure drop in the warm channel is expected to be 4481.67 Pa.

Table 17. Contribution of fluid parameters on pressure drop in the warm channel.

Parameter	Level	Level description	Contribution (Pa)
Mass flow rate (kg/h)	1	20	-13139.00
Gauge outlet pressure (bar)	1	0	-791.00
Inlet temperature (°C)	3	50	-1836.33
Total contributions from all parameters			-15766.33
Current grand average of pressure drop in warm channel			20248
The expected result at optimum conditions			4481.67

4. Conclusions

In this research, the sensitivity analysis of fluid flow parameters on the performance of fully dense ZrB_2-made micro heat exchangers was carried out using the Taguchi approach as a unique and user-friendly optimization method. The most important results of this research can be summarized as follows:

- The average value of pressure drop in the cold channel greatly increases with the increase in mass flow rate.
- A lower pressure drop in the cold channel is appropriate for the better performance of a heat exchanger.
- Mass flow rate is recognized as the main controlling parameter for pressure drop in the cold channel with a significance of ~73%.
- The inlet temperature is identified as the main fluid parameter controlling the warm outlet temperature, with the highest significance of ~72%.
- The warm outlet temperature is very sensitive to the inlet temperature.
- A lower warm outlet temperature is preferred for better heat exchanger performance.
- The cold outlet temperature is very sensitive to inlet temperature, with inlet temperature being the only influential parameter controlling the cold outlet temperature with a significance of ~99%.
- Higher effectiveness is desired for better performance of heat exchangers. Mass flow rate is identified as the main and only controlling parameter for effectiveness, with a significance of ~100%.
- Generally, a lower pressure drop in the warm channel is desired for better performance of heat exchangers.
- Mass flow rate is identified as the main and dominant controlling parameter for pressure drop in the warm channel with a significance of ~97%.

CRediT authorship contribution statement

Mohsen Naderi: Software, Data curation, Visualization, Writing – original draft.
Mohammad Vajdi: Conceptualization, Project administration, Supervision, Writing – review & editing.
Farhad Sadegh Moghanlou: Conceptualization, Supervision, Methodology, Writing – review & editing.
Hossein Nami: Software, Validation, Methodology.

Data availability

The data underlying this article will be shared on reasonable request to the corresponding author.

Declaration of competing interest

The authors declare no competing interests.

Funding and acknowledgment

The authors extend their heartfelt gratitude to the University of Mohaghegh Ardabili for their support of this project, under the auspices of contract No. 1401/D/14/3249, during the completion of Mohsen Naderi's M.Sc. thesis. The resources provided by the University of Southern Denmark have been pivotal in the realization of this work, and the authors sincerely appreciate the institutions commitment to fostering academic excellence and research endeavors.

References

[1] S. Kakaç, H. Liu, A. Pramuanjaroenkij, Heat exchangers: selection, rating, and thermal design, CRC Press, Boca Raton. (2020). https://doi.org/10.1201/9780429469862.
[2] A. Hajatzadeh Pordanjani, S. Aghakhani, M. Afrand, B. Mahmoudi, O. Mahian, S. Wongwises, An updated review on application of nanofluids in heat exchangers for saving energy, Energy Convers. Manag. 198 (2019) 111886. https://doi.org/10.1016/j.enconman.2019.111886.
[3] M.S. Bretado-de los Rios, C.I. Rivera-Solorio, K.D.P. Nigam, An overview of sustainability of heat exchangers and solar thermal applications with nanofluids: A review, Renew. Sustain. Energy Rev. 142 (2021) 110855. https://doi.org/10.1016/j.rser.2021.110855.
[4] B. Alm, U. Imke, R. Knitter, U. Schygulla, S. Zimmermann, Testing and simulation of ceramic micro heat exchangers, Chem. Eng. J. 135 (2008) S179–S184. https://doi.org/10.1016/j.cej.2007.07.005.
[5] R.K. Shah, Research needs in low Reynolds number flow heat exchangers, Heat Transf. Eng. 3 (1981) 49–61. https://doi.org/10.1080/01457638108939580.
[6] S. Wu, J. Mai, Y.C. Tai, C.M. Ho, Micro heat exchanger by using MEMS impinging jets, in Tech. Dig. IEEE Int. MEMS 99 Conf. Twelfth IEEE Int. Conf. Micro Electro Mech. Syst. (Cat. No.99CH36291), IEEE. (1999) 171–176. https://doi.org/10.1109/MEMSYS.1999.746799.
[7] S.A. Ashrafizadeh, Application of second law analysis in heat exchanger systems, Entropy. 21 (2019) 606. https://doi.org/10.3390/e21060606.
[8] S. Nekahi, M. Vajdi, F. Sadegh Moghanlou, K. Vaferi, A. Motallebzadeh, et al., TiB2–SiC-based ceramics as alternative efficient micro heat exchangers, Ceram. Int. 45 (2019) 19060–19067. https://doi.org/10.1016/j.ceramint.2019.06.150.
[9] I.L. Denry, Recent advances in ceramics for dentistry, Crit. Rev. Oral Biol. Med. 7 (1996) 134–143. https://doi.org/10.1177/10454411960070020201.
[10] F. Sadegh Moghanlou, M. Vajdi, M. Sakkaki, S. Azizi, Effect of graphite die geometry on energy consumption during spark plasma sintering of zirconium diboride, Synth. Sinter. 1 (2021) 54–61. https://doi.org/10.53063/synsint.2021.117.
[11] M. Vajdi, F. Sadegh Moghanlou, F. Sharifianjazi, M. Shahedi Asl, M. Shokouhimehr, A review on the Comsol Multiphysics studies of heat transfer in advanced ceramics, J. Compos. Compd. 2 (2020) 35–44. https://doi.org/10.29252/jcc.2.1.5.
[12] A. Sommers, Q. Wang, X. Han, C. T'Joen, Y. Park, A. Jacobi, Ceramics and ceramic matrix composites for heat exchangers in advanced thermal systems—A review, Appl. Therm. Eng. 30 (2010) 1277–1291. https://doi.org/10.1016/j.applthermaleng.2010.02.018.
[13] M. Vajdi, S. Mohammad Bagheri, F. Sadegh Moghanlou, A. Shams Khorrami, Numerical investigation of solar collectors as a potential source for sintering of ZrB2, Synth. Sinter. 1 (2021) 76–84. https://doi.org/10.53063/synsint.2021.128.
[14] M. Shahedi Asl, A. Sabahi Namini, S.A. Delbari, Z. Ahmadi, M. Farvizi, et al., An interfacial survey on the microstructure of ZrB2-based ceramics codoped with carbon fibers and SiC whiskers, Mater. Chem. Phys. 275 (2022) 125322. https://doi.org/10.1016/j.matchemphys.2021.125322.
[15] Z. Ahmadi, M. Shahedi Asl, M. Zakeri, M. Farvizi, On the reactive spark plasma sinterability of ZrB2–SiC–TiN composite, J. Alloys Compd. 909 (2022) 164611. https://doi.org/10.1016/j.jallcom.2022.164611.

[16] A. Shima, M. Kazemi, Influence of TiN addition on densification behavior and mechanical properties of ZrB2 ceramics, Synth. Sinter. 3 (2023) 46–53. https://doi.org/10.53063/synsint.2023.31133.
[17] J.W. Zimmermann, G.E. Hilmas, W.G. Fahrenholtz, R.B. Dinwiddie, W.D. Porter, H. Wang, Thermophysical properties of ZrB2 and ZrB2–SiC ceramics, J. Am. Ceram. Soc. 91 (2008) 1405–1411. https://doi.org/10.1111/j.1551-2916.2008.02268.x.
[18] M. Ghasilzadeh Jarvand, Z. Balak, Oxidation response of ZrB2–SiC–ZrC composites prepared by spark plasma sintering, Synth. Sinter. 2 (2022) 191–197. https://doi.org/10.53063/synsint.2022.24134.
[19] M. Jaberi Zamharir, M. Shahedi Asl, M. Zakeri, M. Razavi, Microstructure of spark plasma coated ultrahigh temperature ZrB2–SiC–Si composites on a graphite substrate, Silicon. 15 (2023) 6015–6024. https://doi.org/10.1007/s12633-023-02475-7.
[20] H. Istgaldi, M. Mehrabian, F. Kazemi, B. Nayebi, Reactive spark plasma sintering of ZrB2-TiC composites: Role of nano-sized carbon black additive, Synth. Sinter. 2 (2022) 67–77. https://doi.org/10.53063/synsint.2022.22107.
[21] D.B. Tuckerman, R.F.W. Pease, High-performance heat sinking for VLSI, IEEE Electron Device Lett. 2 (1981) 126–129. https://doi.org/10.1109/EDL.1981.25367.
[22] P.E.B. Mello, S. Scuotto, F. Ortega, G. Donato, Heat transfer and pressure drop in a plate and fin ceramic heat exchanger, 8th World Conference on Experimental Heat Transfer, Fluid Mechanics and Thermodynamics, Lisbon, Portugal. (2013) 16–20.
[23] T. Fend, W. Völker, R. Miebach, O. Smirnova, D. Gonsior, et al, Experimental investigation of compact silicon carbide heat exchangers for high temperatures, Int. J. Heat Mass Transf. 54 (2011) 4175–4181. https://doi.org/10.1016/j.ijheatmasstransfer.2011.05.028.
[24] M. Fattahi, K. Vaferi, M. Vajdi, F. Sadegh Moghanlou, A. Sabahi Namini, M. Shahedi Asl, Aluminum nitride as an alternative ceramic for fabrication of microchannel heat exchangers: A numerical study, Ceram. Int. 46 (2020) 11647–11657. https://doi.org/10.1016/j.ceramint.2020.01.195.
[25] C.A. Lewinsohn, M.A. Wilson, J.R. Fellows, H.S. Anderson, Fabrication and joining of ceramic compact heat exchangers for process integration, Int. J. Appl. Ceram. Technol. 9 (2012) 700–711. https://doi.org/10.1111/j.1744-7402.2012.02788.x.
[26] N.J. Rathod, M.K. Chopra, U.S. Vidhate, N.B. Gurule, U.V. Saindane, Investigation on the turning process parameters for tool life and production time using Taguchi analysis, Mater. Today Proc. 47 (2021) 5830–5835. https://doi.org/10.1016/j.matpr.2021.04.199.
[27] A. Dwivedi, M. Mohsin Khan, H.S. Pali, Numerical analysis of microchannel heat sink composed of SiC and CNT reinforced ZrB2 composites, J. Eng. Res. 10 (2022) 1–15. https://doi.org/10.36909/jer.18359.
[28] M. Vajdi, M. Shahedi Asl, S. Nekahi, F. Sadegh Moghanlou, S. Jafargholinejad, M. Mohammadi, Numerical assessment of beryllium oxide as an alternative material for micro heat exchangers, Ceram. Int. 46 (2020) 19248–19255. https://doi.org/10.1016/j.ceramint.2020.04.263.
[29] R.K. Shah, D.P. Sekuli, Fundamentals of heat exchanger design, John Wiley & Sons, Inc., Hoboken, NJ, USA. (2003). https://doi.org/10.1002/9780470172605.